Inorganic Chemistry

Article

pubs.acs.org/IC

A Water-Stable Metal–Organic Framework for Highly Sensitive and Selective Sensing of Fe^{3+} Ion

Bing-Lei Hou,[†] Dan Tian,[†] Jiang Liu,[†] Long-Zhang Dong,[†] Shun-Li Li,*[,†] Dong-Sheng Li,[‡] and Ya-Qian Lan*[,†]

[†]School of Chemistry and Materials Science, Nanjing Normal University, Nanjing 210023, P. R. China

[‡]College of Materials and Chemical Engineering, Hubei Provincial Collaborative Innovation Center for New Energy Microgrid, China Three Gorges University, Yichang 443002, P. R. China

Supporting Information

ABSTRACT: A new metal–organic framework $[Zn_5(hfipbb)_4(trz)_2(H_2O)_2]$ (**NNU-1**) [$H_2hfipbb$ = 4,4′-(hexafluoroisopropylidene)bis(benzoic acid), Htrz = 1*H*-1,2,3-triazole] was assembled by hydrothermal synthesis. Single-crystal X-ray diffraction analysis reveals that **NNU-1** displays a twofold interpenetrating three-dimensional (3D) framework with a $\{4^{24}\cdot6^4\}$-**bcu** topology. Interestingly, the 3D framework contains a two-dimensional (2D) layered structure that consists of alternating left- and right-handed double helical chains. On the basis of the hydrophobic $-CF_3$ groups from $H_2hfipbb$ ligand, **NNU-1** possesses excellent stability in water. It is worth noting that **NNU-1** not only shows a highly selective fluorescence quenching effect to Fe^{3+} ion in aqueous solution but also resists the interference of other metals including Fe^{2+} ion. Accordingly, **NNU-1** probably functions as a potential promising fluorescence sensor for detecting Fe^{3+} ion with high sensitivity and selectivity.

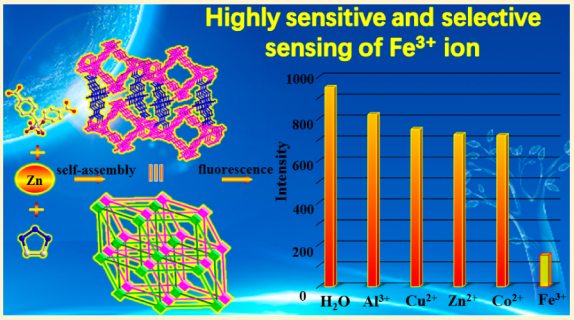

INTRODUCTION

Iron(III) ion not only is an essential metal ion in living organisms but also has a significant impact on a variety of vital cell functions such as muscle function, brain function, and hemoglobin formation.[1] The deficiency and overload of iron(III) ions in an organism can induce various disorders with iron trafficking, storage, and balance being tightly regulated, leading to various health hazards, such as anemia, pathological disorders, and skin ailments.[2] So, how to detect Fe^{3+} ion effectively is an extremely important issue for life system that needs to be given more attention. In spite of various analytical techniques such as spectrophotometry, voltammetry, and atomic absorption spectroscopy having been currently developed for determination of iron(III) ions, it is easily interfered by other metal ions.[3] Thus, it is very necessary to develop novel methods that can be easily applied to exclusively detect Fe^{3+} ion.

Metal–organic frameworks (MOFs) in past few decades have experienced an enormous development due to their intriguing topological frameworks and huge potential applications as functional materials in different realms.[4] For instance, many MOFs have now been considered to be compelling and promising sensors for detecting small inorganic compounds, small organic molecules, and metal ions.[5] This type of sensor commonly displays obvious advantages on the sensitivity, response time, and operability compared with conventional detection means,[6] especially for MOF-supported fluorescent metal ion probes; some significant progress has been made,[7] based on the rational choice of metal ions and organic ligands as well as the structural features (open metal sites, the highly regular channel structures, controllable pore sizes, and so on) of constructed MOFs.[8] Accordingly, MOF-based fluorescent sensor will probably be a judicious choice in efficiently detecting Fe^{3+} ion. Nevertheless, the fact that the poor stability of MOFs in aqueous environment usually largely limits its sensing effect to target metal ions has been verified. Up to now, only a few MOFs-based sensors reported that can maintain their stabilities in water or moist environment.[9] Therefore, improving the water stability of MOFs-based sensors has always been a challenge.[10]

Motivated by the aspects described above, the V-shaped 4,4′-(hexafluoroisopropylidene)bis(benzoic acid) ($H_2hfipbb$) and Zn(II) ions were elaborately chosen as the organic ligands and metal nodes to construct MOF-based fluorescent sensor from the following considerations. On the one hand, the semirigid V-shaped $H_2hfipbb$ ligand was used to construct MOFs with helical structures and various functions such as magnetism, fluorescence, and so on.[11] On the other hand, the $-CF_3$-terminated surface among $H_2hfipbb$ ligand possesses low free energy and the best hydrophobicity, so the MOFs assembled with this ligand may have better water stability. The small 1*H*-1,2,3-triazole (Htrz) molecules (Figure S1) with multidentate coordination sites as auxiliary ligands were also utilized to

Received: July 26, 2016
Published: September 27, 2016

DOI: 10.1021/acs.inorgchem.6b01809
Inorg. Chem. 2016, 55, 10580–10586

increase the interpenetrating possibility of expected helical structure that will be beneficial for the stabilization of MOFs[12] Moreover, Zn^{2+} ions have strong affinity both with carboxylates and Htrz, making it possible to combine H_2hfipbb and Htrz ligands in the same framework. In addition, the metal-carboxylate-azolates are known to have significant water stability, which can further enhance the stabilization of MOFs.[13]

In this work, we report a new three-dimensional (3D) MOF-based sensor, $[Zn_5(hfipbb)_4(trz)_2(H_2O)_2]$ (**NNU-1**) (NNU = Nanjing Normal University), which features an interpenetrating and alternating left- and right-handed double helical structure. As expected, **NNU-1** shows brilliant water stability and excellent fluorescence sensing for Fe^{3+} ion due to fluorescence quenching effect. It is particularly worth mentioning that this effect can be recycled and resist the interference of other metals ions including Fe^{2+}. These results imply that **NNU-1** can completely serve as a good MOF-based fluorescence probe for selective sensing of Fe^{3+} ion.

EXPERIMENTAL SECTION

Materials and General Procedures. All reagents and solvents employed in this work were commercially available and used without further purification. Elemental analyses of C, N, and H were performed on an elemental Vario EL III analyzer. Infrared spectrum using the KBr pellet was measured on a Bruker Tensor 27 in the range of 4000−400 cm^{-1}. Thermogravimetric (TG) analysis was performed on a Netzch STA449F3 analyzer at a heating rate of 5 °C/min from ambient temperature to 800 °C. The room-temperature powder X-ray diffraction (PXRD) spectra were recorded on a Rigaku D/Max 2500/PC diffractometer at 40 kV and 100 mA with a Cu-target tube and a graphite monochromator. Fluorescent spectroscopy data were collected on a Perkin-Elmer LS-50B fluorescence spectrometer. UV−Vis absorption spectra were collected using a Varian Cary 5000 UV−Vis spectrophotometer.

Synthesis. $[Zn_5(hfipbb)_4(trz)_2(H_2O)_2]$ (**NNU-1**). $Zn(NO_3)_2\cdot 6H_2O$ (148.7 mg, 0.5 mmol), H_2hfipbb (39.4 mg, 0.1 mmol), and Htrz (20.0 mg, 0.3 mmol) were added in a mixed solvent of H_2O (3.0 mL) and dimethylformamide (DMF; 1.0 mL), then stirred vigorously for half an hour. The mixture was transferred to a Teflon-lined stainless-steel vessel, then sealed under autogenous pressure at 100 °C for 3 d. After that, it was cooled to room temperature at a rate of 5 °C/min to form colorless needlelike crystals of **NNU-1** (80.2% yield based on H_2hfipbb). Anal. Calcd for $C_{72}H_{40}F_{24}N_6O_{18}Zn_5$ (%): C, 41.98; H, 1.96; N, 4.08. Found (%): C, 41.58; H, 1.79; N, 4.15. IR (KBr pellet, cm^{-1}): 3440 (s), 3153 (w), 3058 (w), 1689 (m), 1616 (s), 1541 (s), 1425 (s), 1400 (s), 1253 (s), 1213 (s), 1174 (s), 1136 (m), 960 (w), 846 (w), 788 (s), 748 (m), 725 (m), 592 (w), 484 (w), 423 (w).

X-ray Crystallography. The single-crystal diffraction data for **NNU-1** were collected on a Bruker AXS smart Apex CCD diffractometer at 296 K. The X-ray generator was operated at 50 kV and 35 mA using Mo Kα (λ = 0.710 73 Å) radiation. The structure was solved by the direct methods of SHELXS-97 and refined by the full-matrix least-squares technique with the SHELXL-97 program.[14] All non-hydrogen atoms were refined with anisotropic temperature parameters. Hydrogen atoms were added theoretically onto the specific atoms and refined isotropically with fixed thermal factors. And some selected bond lengths and angles were listed in Table S1. Crystal data for **NNU-1**: $C_{72}H_{40}F_{24}N_6O_{18}Zn_5$, M_r = 2076.05, monoclinic, a = 20.896 (4) Å, b = 7.3872 (15) Å, c = 31.834 (4) Å, β = 124.636 (9)°, V = 4043.1 (13) $Å^3$, T = 296.15 K, space group $P2/c$, Z = 2, ρ = 1.705 g/cm^3, $F(000)$ = 2064.0, μ = 1.589 mm^{-1}, 25 811 reflection measured, 7100 unique (R_{int} = 0.0801), final R_1 = 0.1108, wR_2 = 0.2086, GOF = 1.065 for all data.

RESULTS AND DISCUSSION

Crystal Structure. Single-crystal X-ray diffraction analysis reveals that **NNU-1** crystallizes in the monoclinic $P2/c$ space group with an asymmetric unit containing three crystallography independent Zn(II) ions, two $hfipbb^{2-}$ ligands, one trz^- ligand, and one coordinated water. As shown in Figure 1, the Zn1 site

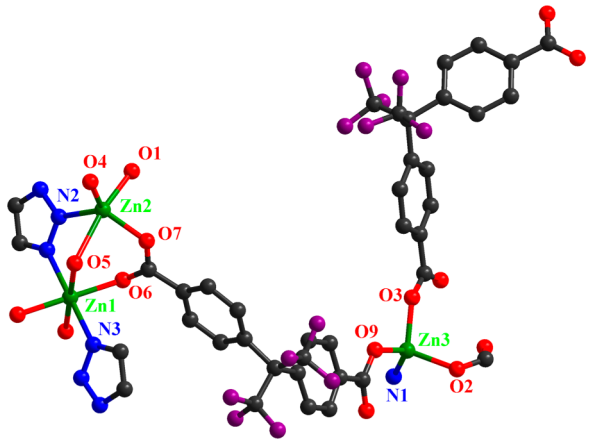

Figure 1. Coordination environments for Zn^{II} atoms in **NNU-1**. (color code: C, black; N, blue; O, red; Zn, green. Hydrogen atoms were omitted for clarity).

is coordinated by two carboxylate oxygen atoms from two $hfipbb^{2-}$ ligands, two nitrogen atoms from two trz^- ligands, and two water molecules, showing a distorted octahedral coordination geometry. The Zn2 site possesses a distorted trigonal bipyramid coordination sphere occupied by one nitrogen atom from one trz^- ligand, three carboxylate oxygen atoms from three $hfipbb^{2-}$ ligands, and one water molecule. The distorted tetrahedral environment of Zn3 site consists of three carboxylate oxygen atoms from three $hfipbb^{2-}$ ligands and one nitrogen atom from one trz^- ligand. The Zn−O and Zn−N bond lengths are all within the normal ranges.[15] Two kinds of $hfipbb^{2-}$ ligands show the completely identical coordination modes with monodentate and bidentate types. And trz^- ligand acts as a tridentate ligand to connect three kinds of Zn atoms (Figure S1). Notably, a distorted Zn1 octahedron links with two distorted Zn2 trigonal bipyramids by sharing the same vertex to form a txrinuclear $\{Zn_3\}$ cluster, which is further fixed by two carboxylic groups, two water molecules, and two trz^- ligands. And then each $\{Zn_3\}$ cluster connects two adjacent Zn3 tetrahedra to build a pentanuclear $\{Zn_5\}$ cluster bridged by carboxylate groups and trz^- ligands (Figure S2). First, one kind of $hfipbb^{2-}$ ligand links $\{Zn_5\}$ clusters along the crystallographic c axis to form an undulating 2D network having a large rhomblike window with the dimensions of 7.84 × 15.67 $Å^2$ (Figure S3). A layered structure is formed by the penetration of two such identical networks (Figure 2a−c). In detail, the structure is catenated with two kinds of well-organized rings (Figure 2d). Interestingly, the layered structure consists of alternating left- and right-handed double helical chains (Figure S4) by sharing the $\{Zn_5\}$ clusters (Figure S5). Second, the other kind of $hfipbb^{2-}$ ligand extends such undulating 2D networks to yield a 3D framework (Figure S6). Remarkably, owing to the presence of enough space, two such frameworks interweave into a twofold interpenetrating array (Figure 2e,f). A better insight into the nature of **NNU-1** can be achieved by regarding each $\{Zn_5\}$ cluster as an eight-connected node and

DOI: 10.1021/acs.inorgchem.6b01809
Inorg. Chem. 2016, 55, 10580−10586

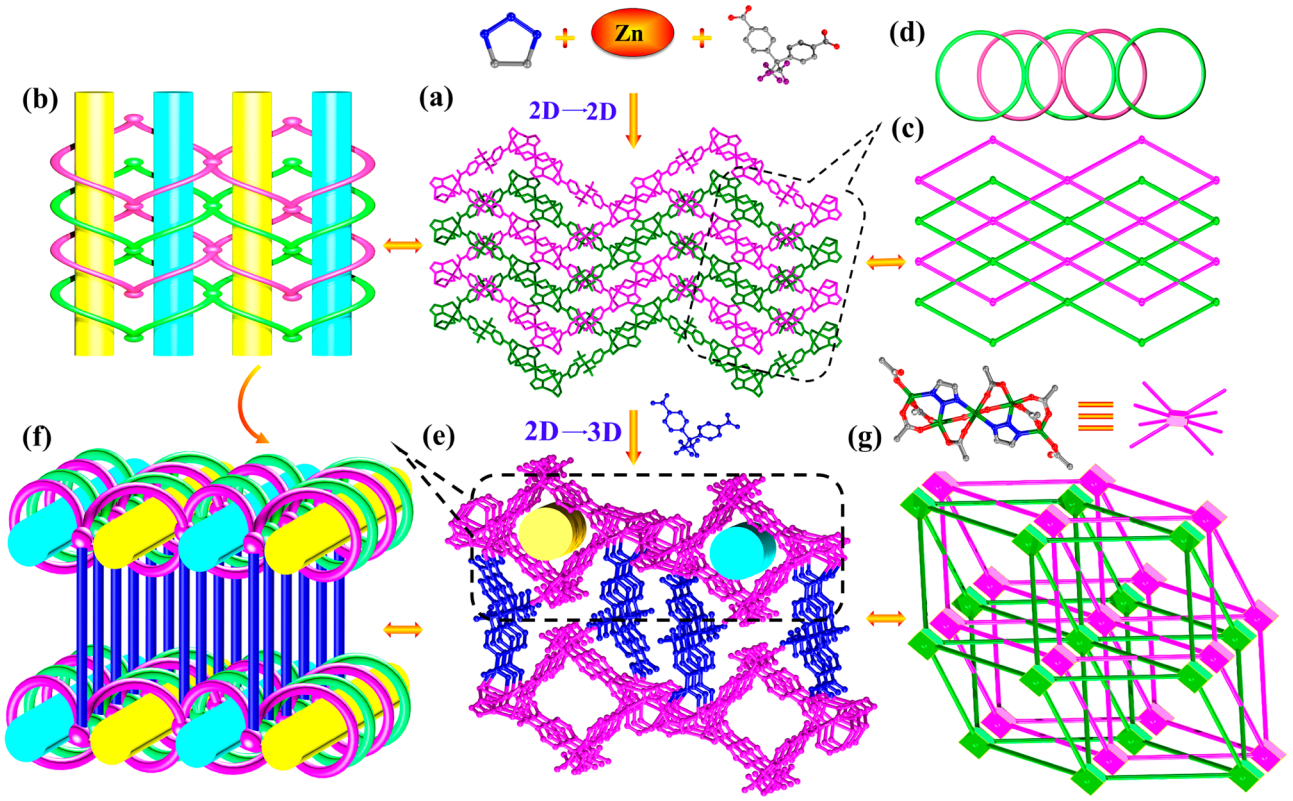

Figure 2. (a) Wires or stick representation of the 2D structure of **NNU-1**. (b) Schematic view of the twofold interpenetrating 2D layer. (c) Schematic view of the topological structure of twofold interpenetrating 2D layer in **NNU-1**. (d) Schematic view of the twofold interpenetrating in the 2D layer. (e) Ball-and-stick representation of the 3D structure of **NNU-1**. (f) Schematic view of the 3D structure of **NNU-1**. (g) Polyhedron schematic view of the topological structure of **NNU-1**.

the $hfipbb^{2-}$ ligand as a linear linker. The simplified structure of **NNU-1** is a twofold interpenetrating **bcu** topology with Schläfli symbol $\{4^{24}\cdot6^{4}\}$ (Figure 2g), which was determined by TOPOS.[16] Offering further analysis of this interesting high connected network topology, the utilization of multidentate bridging ligand trz^{-} and carboxylate ligand with various coordination modes effectively led to a high connected node $\{Zn_5\}$ cluster. In addition, the semirigid V-shaped carboxylate ligand is conducive to form the interpenetrating structure. Previous examples of eight-connected framework are commonly composed of Co, Cd, Cu atoms and so on.[17] There are few reports on the construction of Zn-MOFs with eight connections. Recently, Long Chen et al. have enumerated an eight-connected net based on two different trinuclear $\{Zn_3\}$ secondary building units, and the FDA^{2-} serves as bridging linker.[18] In this case, **NNU-1** is clearly different from the previous, where the $\{Zn_5\}$ cluster as an eight-connected node and the semirigid V-shaped $hfipbb^{2-}$ as bridging linkers to form the **bcu** net. Moreover, two **bcu** nets interweave into a two-fold interpenetrating network that is rarely reported before. In all, according to the topological analysis results, selecting semirigid V-shaped ligand and suitable secondary ligand in the reaction system can effectively form the novel structure.

Stability of NNU-1. Most MOFs with weak metal−ligand coordination bonds are more or less vulnerable to water molecules under an ambient atmospheric environment and, consequently, not suitable for many industrial applications.[19] Therefore, it is significant to construct MOFs with excellent water stability for expanding their practical applications. The $-CF_3$-terminated surface among $H_2hfipbb$ ligand was reported to possess low free energy and the best hydrophobicity,[20] so we hope to construct an MOF with excellent moisture/water tolerance by using $H_2hfipbb$ ligand. Fortunately, **NNU-1** was synthesized, and it can be stable in water for 7 d at least at room temperature, while it is unexpected that **NNU-1** can be stable in the boiling water for 72 h. To further investigate the chemical stability of **NNU-1**, the sample was immerged in different pH solutions for 24 h, and the identity PXRD pattern before and after immerged demonstrated that the framework possesses excellent pH stability (Figure S9). In addition, **NNU-1** is stable in some other solvents, such as CH_3OH, CH_3CH_2OH, $(CH_3)_2CHOH$, DMF, dimethylacetamide (DMA), CH_2Cl_2, $CHCl_3$, tetrahydrofuran, CH_3CN, and CH_3COCH_3 at room temperature. The PXRD patterns of the as-synthesized **NNU-1** and **NNU-1** in water and different organic solvents match well with that simulated from the single-crystal data, showing the excellent stabilities of **NNU-1** in these conditions (Figures 3a and S10).

Fluorescence Properties for Sensing Metal Ions. Metal−organic frameworks with d^{10} transition metal ions have attracted intense interest from chemists owing to their potential applications in photoactive materials.[21] Thereby, the fluorescence properties of NNU-1 and $H_2hfipbb$ ligand were investigated in the solid state. The fluorescence spectra of the free $H_2hfipbb$ ligand and the as-synthesized **NNU-1** show strong broad emission bands centered at 404 and 406 nm in the solid state under the same excitation at 260 nm (Figure S11), which may be attributed to the $\pi^*-\pi$ transitions and the $H_2hfipbb$ intraligand charge transfer, respectively.[22] In addition, the fluorescence properties of **NNU-1** (5.0 mg) in different

DOI: 10.1021/acs.inorgchem.6b01809
Inorg. Chem. 2016, 55, 10580−10586

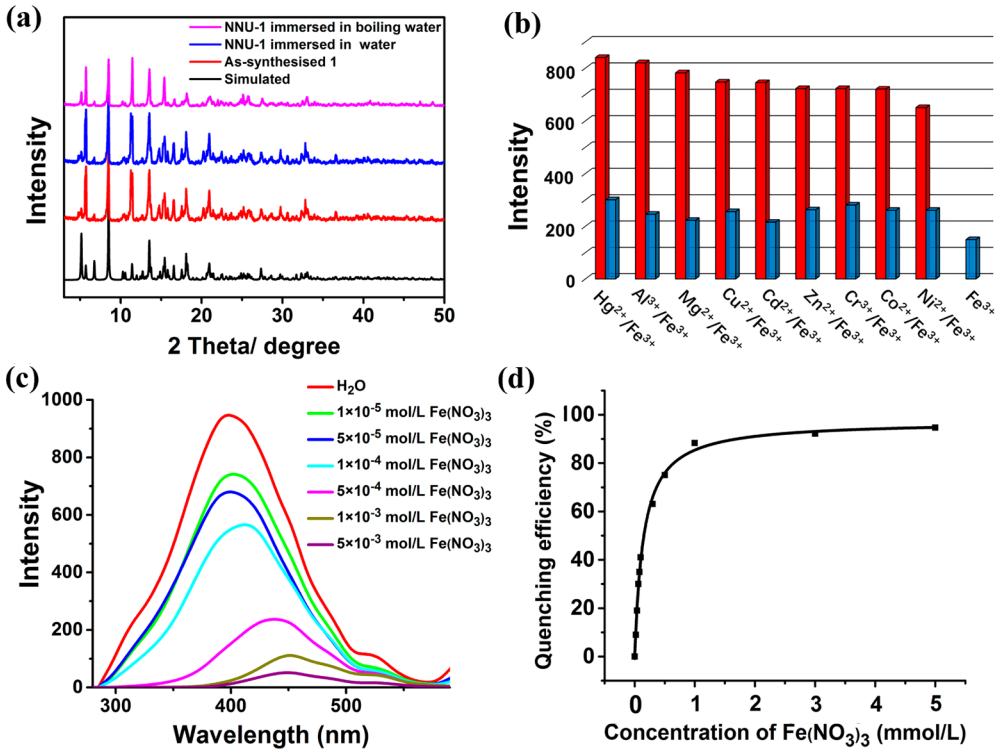

Figure 3. (a) PXRD patterns of simulated, as-synthesized, **NNU-1** immersed in water at room temperature and in boiling water for 72 h. (b) Fluorescence intensities of **NNU-1** immersed in the individual aqueous solutions of $M(NO_3)_x$ (1×10^{-3} mol·L^{-1}; red color) and mixed metal ions including Fe^{3+} ion (1×10^{-3} mol·L^{-1}; blue color) under an excitation of 260 nm. (c) Variation of fluorescence intensities of **NNU-1** immersed in the aqueous solutions with different concentrations of $Fe(NO_3)_3$ (λ_{ex} = 260 nm). (d) The relationship between the quenching efficiency and the amount of Fe^{3+} ion.

liquid suspension (3.0 mL) were investigated. The results obtained (Figure S12) showed that the fluorescence intensity and varying shifts of **NNU-1** in different suspensions are dependent on the solvent nature, and the strongest emission is observed in its aqueous solution.

Owing to the excellent fluorescence property and water stability, **NNU-1** has attracted our interest to explore its application in sensing metal ions in aqueous solution. To investigate the ability of selective sensing of metal ions, **NNU-1** (5.0 mg) was ground and immersed in the individual aqueous solutions of $M(NO_3)_x$ (3.0 mL, 0.001 mol·L^{-1}, M = Mg^{2+}, Cr^{3+}, Cu^{2+}, Ni^{2+}, Cd^{2+}, Zn^{2+}, Co^{2+}, Al^{3+}, Fe^{3+}, and Hg^{2+}, respectively) for 1 d to form uniform dispersion suspensions for fluorescence study.[23] As presented in Figure 3b, there exists an obvious quenching effect to Fe^{3+} ion upon the fluorescence intensity of **NNU-1** excited at 260 nm. The anti-interference sensing experiments were further conducted. **NNU-1** (5.0 mg) was immersed in aqueous solutions containing mixed Fe^{3+} ion and other metal ions (Mg^{2+}, Cr^{3+}, Cu^{2+}, Ni^{2+}, Cd^{2+}, Zn^{2+}, Co^{2+}, Al^{3+}, Hg^{2+}) with a concentration of 1×10^{-3} M. Therein, the mixed addition of other metal ions only resulted in a slight reduction in fluorescence intensity, and the emission is quenched only after the addition of Fe^{3+} ion, verifying that the Fe^{3+} ion can still be sensed in the presence of several other metal ions (Figure 3b). Moreover, a reversible processing was performed: **NNU-1** is immersed in aqueous solution of $Fe(NO_3)_3$ for 24 h and then is centrifuged and washed with aqueous solution until the solution is colorless. Strong fluorescence intensity is observed after three sensing−recovery cycles (Figure S13). Meanwhile, PXRD pattern of **NNU-1** after this treatment matched well with the simulated one as well as the as-synthesized one (Figure S14). In view of the above-mentioned superior fluorescent sensing properties of **NNU-1**, this crystal material may act as a potentially practical fluorescence sensor for detecting Fe^{3+} ion with high reversibility.

It is normal to take Fe^{2+} into consideration, and fluorescence properties of **NNU-1** in different aqueous solutions containing either Fe^{3+} or Fe^{2+} were investigated. Fe^{3+} salts have upper quenching efficiency for **NNU-1**, while Fe^{2+} salts show lower quenching efficiency (Figure S15). This phenomenon not only indicated that the intensity quenching is not dependent on the anions (i.e., Cl^- and SO_4^{2-}) but also showed that there is no disturbance on selective sensing of Fe^{3+} ion in the presence of Fe^{2+} ion. In brief, **NNU-1** shows highly selective sensing ability for Fe^{3+} ion in the presence of other metals including Fe^{2+} ion.

To further assess sensing sensitivity toward Fe^{3+} ion, a batch of suspensions of **NNU-1** with gradually increasing Fe^{3+} concentration in water from 1×10^{-5} to 5×10^{-3} mol·L^{-1} were prepared to test the emissive response. The emission intensity of **NNU-1** excited at 260 nm was gradually quenched with addition of increasing concentrations of Fe^{3+} (Figure 3c). A significant red shift (40 nm) was observed accompanied by the increasing Fe^{3+} concentration, which may be caused by the solvatochromism effect.[24] In detail, the relationship between the quenching efficiency and the amount of Fe^{3+} ion is illustrated in Figure 3d. The quenching efficiency could reach 96.60%, while the concentration reaches 5×10^{-3} mol·L^{-1}, which is comparable to other reported excellent sensors for responding to Fe^{3+} (Table S2) Moreover, there exists a good linear correlation (R^2 = 0.980) between the quenching efficiency and the amount of Fe^{3+} ion in the low concentration range of 0−0.1 mmol·L^{-1} (Figure S16). Meanwhile, the

DOI: 10.1021/acs.inorgchem.6b01809
Inorg. Chem. 2016, 55, 10580−10586

detection limit calculated with $3\sigma/k$ (k: slope, σ: standard error) is ~0.20 mmol·L^{-1}, which is a clear point of high sensing sensitivity of **NNU-1** for Fe^{3+} ion.[25] It is apparent that **NNU-1** features highly sensitive sensing ability for Fe^{3+} ion. On the basis of the above pieces of evidence, **NNU-1** may be a practical promising fluorescence sensor for detecting Fe^{3+} ion with high selectivity and sensitivity.

The Underlying Mechanism of Luminescence Quenching. The underlying mechanism of luminescence quenching by Fe^{3+} ion was further investigated in detail. First, considering the collapse of the framework, the PXRD was measured after this sample immersed in metal ion solutions. As confirmed by PXRD patterns (Figure S14), the crystal structure of **NNU-1** immersed in metal ion solutions remains unchanged, showing that this quenching phenomenon has no relation with the framework of the crystal. Second, the resonance energy transfer was another possible reason for the quenching phenomena. If the emission spectrum of the fluorophore (donor) has a certain degree of overlap with the absorption band of the analyte (acceptor), when the distance between them is appropriate, the resonance energy transfer can be observed from the donor to the acceptor.[23] Therefore, the UV−vis absorption spectra for $M(NO_3)_x$ suspensions containing different metal ions (1×10^{-3} mol·L^{-1}) were investigated, respectively. An inappreciable spectral overlap between the absorption spectrum of Fe^{3+} aqueous solution and the emission peaks of **NNU-1** was observed (Figure S17). However, the absorption spectrum of Fe^{3+} aqueous solution has a majority of overlaps with the excitation spectrum of **NNU-1**, while other metal ion solutions have no obvious overlaps. The above results indicate that this quenching phenomenon may be attributed to the competition absorption of the excitation wavelength (332 nm) energy between Fe^{3+} aqueous solution and **NNU-1**. In addition, a series of UV−vis absorption spectra were measured upon a gradually increasing concentration of $Fe(NO_3)_3$ and accompanied by a monotonically increasing trend of absorption intensity (Figure S18). Notably, this result is consistent with the tendency of the quenching efficiency. In consideration of these pieces of evidence, we then draw the conclusion that the competitive absorption mechanism may be responsible for the quenching effect, as reported in other literature reports.[26]

CONCLUSION

In summary, a new water-stable MOF (**NNU-1**) was successfully synthesized under solvothermal conditions with a twofold interpenetrating three-dimensional framework. Importantly, **NNU-1** can retain its crystal structure in water, even boiling water, and exhibit a highly sensitive and selective fluorescence quenching effect to Fe^{3+} ion in aqueous solutions. It is significant that **NNU-1** can resist the interference from other metal ions including Fe^{2+} ion and be used reversibly. Further experiments and studies in regard to mechanisms indicated that the competitive absorption of excitation wavelength energy between Fe^{3+} ion and **NNU-1** results in the quenching effect. Clearly, this work provides a new water-stable MOF with functional groups that possesses a significant potential ability as a highly sensitive and selective sensor for sensing Fe^{3+} ion, which makes the **NNU-1** a potential candidate for applications in fluorescence probes and biological detection. In brief, the present work opens a promising approach to design MOF-based sensors for Fe^{3+} ion; this will probably be useful under more realistic conditions and broader scope in the future.

ASSOCIATED CONTENT

Supporting Information

The Supporting Information is available free of charge on the ACS Publications website at DOI: 10.1021/acs.inorgchem.6b01809.

IR spectrum, TG curve, PXRD patterns, fluorescence spectra, UV−vis adsorption spectra (PDF)
Crystallographic details (CIF)

AUTHOR INFORMATION

Corresponding Authors

*E-mail: yqlan@njnu.edu.cn. (Y.-Q.L.)
*E-mail: slli@njnu.edu.cn. (S.-L.L.)

Notes

The authors declare no competing financial interest.

ACKNOWLEDGMENTS

This work was financially supported by the National Natural Science Foundation of China (Nos. 21371099 and 21471080), the NSF of Jiangsu Province of China (Nos. BK20130043 and BK20141445), the Priority Academic Program Development of Jiangsu Higher Education Institutions, and the Foundation of Jiangsu Collaborative Innovation Center of Biomedical Functional Materials.

REFERENCES

(1) (a) Bricks, J. L.; Kovalchuk, A.; Trieflinger, C.; Nofz, M.; Buschel, M.; Tolmachev, A. I.; Daub, J.; Rurack, K. On the Development of Sensor Molecules that Display Fe^{III}-amplified Fluorescence. *J. Am. Chem. Soc.* **2005**, *127*, 13522−13529. (b) Chen, B.; Yang, Y.; Zapata, F.; Lin, G.; Qian, G.; Lobkovsky, E. B. Luminescent Open Metal Sites within a Metal−Organic Framework for Sensing Small Molecules. *Adv. Mater.* **2007**, *19*, 1693−1696. (c) Zheng, M.; Tan, H. Q.; Xie, Z. G.; Zhang, L. G.; Jing, X. B.; Sun, Z. C. Fast Response and High Sensitivity Europium Metal Organic Framework Fluorescent Probe with Chelating Terpyridine Sites for Fe^{3+}. *ACS Appl. Mater. Interfaces* **2013**, *5*, 1078−1083.

(2) (a) Barba-Bon, A.; Costero, A. M.; Gil, S.; Parra, M.; Soto, J.; Martinez-Manez, R.; Sancenon, F. A New Selective Fluorogenic Probe for Trivalent Cations. *Chem. Commun.* **2012**, *48*, 3000−3002. (b) Kawano, T.; Kadono, T.; Furuichi, T.; Muto, S.; Lapeyrie, F. Aluminum-induced Distortion in Calcium Signaling Involving Oxidative Bursts and Channel Regulation in Tobacco BY-2 Cells. *Biochem. Biophys. Res. Commun.* **2003**, *308*, 35−42. (c) Andrews, N. C. Disorders of Iron Metabolism. *N. Engl. J. Med.* **1999**, *341*, 1986−1995.

(3) (a) Chen, Z.; Sun, Y.; Zhang, L.; Sun, D.; Liu, F.; Meng, Q.; Wang, R.; Sun, D. A Tubular Europium−Organic Framework Exhibiting Selective Sensing of Fe^{3+} and Al^{3+} Over Mixed Metal Ions. *Chem. Commun.* **2013**, *49*, 11557−11559. (b) Ohashi, A.; Ito, H.; Kanai, C.; Imura, H.; Ohashi, K. Cloud Point Extraction of Iron(III) and Vanadium(V) Using 8-quinolinol Derivatives and Triton X-100 and Determination of 10^{-7} mol dm^{-3} level Iron(III) in Riverine Water Reference by a Graphite Furnace Atomic Absorption Spectroscopy. *Talanta* **2005**, *65*, 525−530. (c) Elrod, V. A.; Johnson, K. S.; Coale, K. H. Determination of Subnanomolar Levels of Iron(II) and Total Dissolved Iron in Seawater by Flow Injection and Analysis with Chemiluminescence Detection. *Anal. Chem.* **1991**, *63*, 893−898. (d) Tesfaldet, Z. O.; van Staden, J. F.; Stefan, R. I. Sequential Injection Spectrophotometric Determination of Iron as Fe(II) in Multi-vitamin Preparations Using 1,10-phenanthroline as Complexing Agent. *Talanta* **2004**, *64*, 1189−1195.

(4) (a) Heine, J.; Muller-Buschbaum, K. Engineering Metal-based Luminescence in Coordination Polymers and Metal−Organic Frameworks. *Chem. Soc. Rev.* **2013**, *42*, 9232−9242. (b) Zhao, Q.; Li, F.; Huang, C. Phosphorescent Chemosensors Based on Heavy-Metal

DOI: 10.1021/acs.inorgchem.6b01809
Inorg. Chem. 2016, 55, 10580−10586

Complexes. *Chem. Soc. Rev.* **2010**, *39*, 3007−3030. (c) Tsukanov, A. V.; Dubonosov, A. D.; Bren, V. A.; Minkin, V. I. Organic Chemosensors with Crown-ether Groups. *Chem. Heterocycl. Compd.* **2008**, *44*, 899−923. (d) Prodi, L.; Balletta, F.; Mantalti, M.; Zaccheroni, N. Luminescent Chemosensors for Transition Metal Ions. *Coord. Chem. Rev.* **2000**, *205*, 59−83. (e) Williams, D. E.; Rietman, J. A.; Maier, J. M.; Tan, R.; Greytak, A. B.; Smith, M. D.; Krause, J. A.; Shustova, N. B. Energy Transfer on Demand: Photoswitch-Directed Behavior of Metal−Porphyrin Frameworks. *J. Am. Chem. Soc.* **2014**, *136*, 11886−11889. (f) Lu, W. G.; Wei, Z. W.; Gu, Z. Y.; Liu, T. F.; Park, J.; Park, J.; Tian, J.; Zhang, M. W.; Zhang, Q.; Gentle, T., III; Bosch, M.; Zhou, H. C. Tuning the Structure and Function of Metal−Organic Frameworks via Linker Design. *Chem. Soc. Rev.* **2014**, *43*, 5561−5593. (g) Qiu, S. L.; Xue, M.; Zhu, G. S. Metal−organic Framework Membranes: from Synthesis to Separation Application. *Chem. Soc. Rev.* **2014**, *43*, 6116−6140.

(5) (a) Hao, Z.; Song, X.; Zhu, M.; Meng, X.; Zhao, S.; Su, S.; Yang, W.; Song, S.; Zhang, H. One-dimensional Channel-structured Eu-MOF for Sensing Small Organic Molecules and Cu^{2+} Ion. *J. Mater. Chem. A* **2013**, *1*, 11043−11050. (b) Dang, S.; Ma, E.; Sun, Z. M.; Zhang, H. A Layer-structured Eu-MOF as a Highly Selective Fluorescent Probe for Fe^{3+} Detection Through a Cation-exchange Approach. *J. Mater. Chem.* **2012**, *22*, 16920−16926.

(6) (a) Xu, H.; Gao, J.; Qian, X.; Wang, J.; He, H.; Cui, Y.; Yang, Y.; Wang, Z.; Qian, G. Metal−Organic Framework Nanosheets for Fast-response and Highly Sensitive Luminescent Sensing of Fe^{3+}. *J. Mater. Chem. A* **2016**, *4*, 10900−10905. (b) Kong, D.; Yan, F.; Han, Z.; Xu, J.; Guo, X.; Chen, L. Cobalt(II) Ions Detection using Carbon Dots as an Sensitive and Selective Fluorescent Probe. *RSC Adv.* **2016**, *6*, 67481−67487.

(7) (a) Wang, J.; He, C.; Wu, P.; Wang, J.; Duan, C. An Amide-containing Metal−Organic Tetrahedron Responding to a Spin-trapping Reaction in a Fluorescent Enhancement Manner for Biological Imaging of NO In Living. *J. Am. Chem. Soc.* **2011**, *133*, 12402−12405. (b) Hu, Z.; Deibert, B. J.; Li, J. Luminescent Metal−Organic Frameworks for Chemical Sensing and Explosive Detection. *Chem. Soc. Rev.* **2014**, *43*, 5815−5840.

(8) (a) Das, M. C.; Xiang, S. C.; Zhang, Z. J.; Chen, B. L. Funktionelle Gemischtmetall−Organische Gerüste mit Metalloliganden. *Angew. Chem.* **2011**, *123*, 10696−10707. (b) Wong, K. L.; Law, G. L.; Yang, Y. Y.; Wong, W. T. A Highly Porous Luminescent Terbium−Organic Framework for Reversible Anion Sensing. *Adv. Mater.* **2006**, *18*, 1051−1054. (c) Li, Y.; Zhang, S. S.; Song, D. T. A Luminescent Metal−Organic Framework as a Turn-On Sensor for DMF Vapor. *Angew. Chem.* **2013**, *125*, 738−741. (d) Takashima, Y.; Martinez, V. M.; Furukawa, S.; Kondo, M.; Shimomura, S.; Uehara, H.; Nakahama, M.; Sugimoto, K.; Kitagawa, S. Molecular Decoding using Luminescence from an Entangled Porous Framework. *Nat. Commun.* **2011**, *2*, 168−176.

(9) (a) Jiang, H. L.; Feng, D.; Gu, Z. Y.; Wei, Z.; Chen, Y. P.; Zhou, H. C.; et al. An Exceptionally Stable, Porphyrinic Zr Metal−Organic Framework Exhibiting pH-Dependent Fluorescence. *J. Am. Chem. Soc.* **2013**, *135*, 13934−13938. (b) Yang, Q.; Vaesen, S.; Ragon, F.; Wiersum, A. D.; Wu, D.; Lago, A.; Devic, T.; Martineau, C.; Taulelle, F.; Llewellyn, P. L.; Jobic, H.; Zhong, C.; Serre, C.; de Weireld, G.; Maurin, G. A Water Stable Metal−Organic Framework with Optimal Features for CO_2 Capture. *Angew. Chem., Int. Ed.* **2013**, *52*, 10316−10320.

(10) (a) Zhang, W.; Hu, Y.; Ge, J.; Jiang, H. L.; Yu, S. H. A Facile and General Coating Approach to Moisture/Water-Resistant Metal−Organic Frameworks with Intact Porosity. *J. Am. Chem. Soc.* **2014**, *136*, 16978−16981. (b) Wang, M.; Zhang, G.; Zhang, D.; Zhu, D.; Tang, B. Z. Fluorescent Bio/chemosensors based on Silole and Tetraphenylethene Luminogens with Aggregation-induced Emission Feature. *J. Mater. Chem.* **2010**, *20*, 1858−1867. (c) Chen, B. L.; Wang, L. B.; Xiao, Y. Q.; Fronczek, F. R.; Xue, M.; Cui, Y. J.; Qian, G. A Luminescent Metal−Organic Framework with Lewis Basic Pyridyl Sites for the Sensing of Metal Ions. *Angew. Chem., Int. Ed.* **2009**, *48*, 500−503.

(11) (a) Banerjee, R.; Phan, A.; Wang, B.; Knobler, C.; Furukawa, H.; O'Keeffe, M.; Yaghi, O. M. High-throughput Synthesis of Zeolitic Imidazolate Frameworks and Application to CO_2 Capture. *Science* **2008**, *319*, 939−943. (b) Li, J. R.; Sculley, J.; Zhou, H. C. Metal−Organic Frameworks for Separations. *Chem. Rev.* **2012**, *112*, 869−932. (c) Lee, J.; Farha, O. K.; Roberts, J.; Scheidt, K. A.; Nguyen, S. T.; Hupp, J. T. Metal−organic Framework Materials as Catalysts. *Chem. Soc. Rev.* **2009**, *38*, 1450−1459. (d) Corma, A.; García, H.; Llabrés i Xamena, F. X. L. Engineering Metal Organic Frameworks for Heterogeneous Catalysis. *Chem. Rev.* **2010**, *110*, 4606−4655. (e) Kurmoo, M. Magnetic Metal−Organic Frameworks. *Chem. Soc. Rev.* **2009**, *38*, 1353−1379. (f) Heine, J.; Muller-Buschbaum, K. Engineering Metal-based Luminescence in Coordination Polymers and Metal−Organic Frameworks. *Chem. Soc. Rev.* **2013**, *42*, 9232−9242.

(12) (a) Brotherton, W. S.; Guha, P. M.; Phan, H.; Clark, R. J.; Shatruk, M.; Zhu, L. Tridentate Complexes of 2,6-bis(4-substituted-1,2,3-triazol-1-ylmethyl)pyridine and its Organic Azide Precursors: An Application of the Copper(II) Acetate-accelerated Azide−alkyne Cycloaddition. *Dalton Trans.* **2011**, *40*, 3655−3665. (b) Anderson, C. B.; Elliott, A. B. S.; Lewis, J. E. M.; McAdam, C. J.; Gordon, K. C.; Crowley, J. D. Fac-Re$(CO)_3$ Complexes of 2,6-bis(4-substituted-1,2,3-triazol-1-ylmethyl)pyridine "click" Ligands: Synthesis, Characterisation and Photophysical Properties. *Dalton Trans.* **2012**, *41*, 14625−14632. (c) Miguel-Fernandez, S.; Martinez de Salinas, S.; Diez, J.; Gamasa, M. P.; Lastra, E. 1, 3-Dipolar Cycloadditions of Ruthenium(II) Azido Complexes with Alkynes and Nitriles. *Inorg. Chem.* **2013**, *52*, 4293−4302.

(13) Zheng, S. T.; Wu, T.; Zhang, J.; Chow, M.; Nieto, R. A.; Feng, P. Y.; Bu, X. H. Porous Metal Carboxylate Boron Imidazolate Frameworks. *Angew. Chem., Int. Ed.* **2010**, *49*, 5362−5366.

(14) Sheldrick, G. M. *SHELXTL NT,* Version 5.1, Program for solution and refinement of crystal structures; University of Göttingen: Germany, 1997.

(15) Zhang, J. P.; Lin, Y. Y.; Huang, X. C.; Chen, X. M. Designed Assembly and Structures and Photoluminescence of a New Class of Discrete Zn^{II} Complexes of 1H-1,10-Phenanthroline-2-one. *Eur. J. Inorg. Chem.* **2006**, *2006*, 3407−3412.

(16) (a) Sheldrick, G. M. Crystal Structure Refinement with SHELXL, *Acta Crystallogr.* Sect. C. *Acta Crystallogr., Sect. C: Struct. Chem.* **2015**, *71*, 3−8. (b) Blatov, V. A.; Shevchenko, A. P.; Proserpio, D. M. Applied Topological Analysis of Crystal Structures with the Program Package ToposPro. *Cryst. Growth Des.* **2014**, *14*, 3576−3586.

(17) (a) Goswami, S.; Sanda, S.; Konar, S. A Porous Metal Organic Framework with a bcu-type Topology Involving in Situ Ligand Formation−synthesis, Structure, Magnetic Property and Gas Adsorption Studies. *CrystEngComm* **2014**, *16*, 369−374. (b) Lin, H. M.; Chang, T. Y. A Three-Dimensional Porous Metal−Organic Framework with a Body-Centered Cubic Topology Constructed from 48-Membered Tetraicosanuclear Metallamacrocycle Based on in Situ Ligand Synthesis. *Cryst. Growth Des.* **2009**, *9*, 2988−2990. (c) Liu, S.; Gao, H. L.; Cui, J. Z. A New 3D Metal−Organic Framework Based on a Hexanuclear Cobalt (II): Synthesis, Structure, and Magnetic Property. *Inorg. Chem. Commun.* **2015**, *55*, 14−16.

(18) Li, H. H.; Niu, Z.; Chen, L.; Jiang, H. B.; Wang, Y. P.; Cheng, P. Three Luminescent Metal−Organic Frameworks Constructed from Trinuclear Zinc(II) Clusters and furan-2,5-dicarboxylate. *CrystEngComm* **2015**, *17*, 5101−5109.

(19) Low, J. J.; Benin, A. I.; Jakubczak, P.; Abrahamian, J. F.; Faheem, S. A.; Willis, R. R. Virtual High Throughput Screening Confirmed Experimentally: Porous Coordination Polymer Hydration. *J. Am. Chem. Soc.* **2009**, *131*, 15834−15842.

(20) (a) Nishino, T.; Meguro, M.; Nakamae, K.; Matsushita, M.; Ueda, Y. The Lowest Surface Free Energy Based on − CF_3 Alignment. *Langmuir* **1999**, *15*, 4321−4323. (b) Sun, T.; Qing, G.; Su, B.; Jiang, L. Functional Biointerface Materials Inspired from Nature. *Chem. Soc. Rev.* **2011**, *40*, 2909−2921.

(21) (a) Rocha, J.; Carlos, L. D.; Paz, F. A. A.; Ananias, D. Luminescent Multifunctional Lanthanides-based Metal−Organic Frameworks. *Chem. Soc. Rev.* **2011**, *40*, 926−940. (b) Allendorf, M.

DOI: 10.1021/acs.inorgchem.6b01809
Inorg. Chem. 2016, 55, 10580−10586

D.; Bauer, C. A.; Bhakta, R. K.; Houk, R. J. T. Luminescent Metal−Organic Frameworks. *Chem. Soc. Rev.* **2009**, *38*, 1330−1352.
(22) (a) Gao, J. Y.; Wang, N.; Xiong, X. H.; Chen, C. J.; Xie, W. P.; Ran, X. R.; Long, Y.; Yue, S. T.; Liu, Y. L. Syntheses, Structures, and Photoluminescent Properties of a Series of Zinc(II)−3-amino-1,2,4-triazolate Coordination Polymers Constructed by Varying Carboxylate Anions. *CrystEngComm* **2013**, *15*, 3261−3270. (b) Zhang, L. Y.; Liu, G. F.; Zheng, S. L.; Ye, B. H.; Zhang, X. M.; Chen, X. M. Helical Ribbons of Cadmium(II) and Zinc(II) Dicarboxylates with Bipyridyl-Like Chelates − Syntheses, Crystal Structures and Photoluminescence. *Eur. J. Inorg. Chem.* **2003**, *2003*, 2965−2971. (c) Guo, X. D.; Zhu, G. S.; Sun, F. X.; Li, Z. Y.; Zhao, X. J.; Li, X. T.; Wang, H. C.; Qiu, S. L. Synthesis, Structure, and Luminescent Properties of Microporous Lanthanide Metal-Organic Frameworks with Inorganic Rod-shaped Building Units. *Inorg. Chem.* **2006**, *45*, 2581−2587.
(23) Zhang, S. R.; Du, D. Y.; Qin, J. S.; Bao, S. J.; Li, S. L.; He, W. W.; Lan, Y. Q.; Shen, P.; Su, Z. M. A Fluorescent Sensor for Highly Selective Detection of Nitroaromatic Explosives Based on a 2D, Extremely Stable, Metal−Organic Framework. *Chem. - Eur. J.* **2014**, *20*, 3589−3594.
(24) (a) Hu, F. L.; Shi, Y. X.; Chen, H. H.; Lang, J. P. A Zn(II) Coordination Polymer and its Photocycloaddition Product: Syntheses, Structures, Selective Luminescence Sensing of Iron(III) Ions and Selective Absorption of Dyes. *Dalton Trans.* **2015**, *44*, 18795−18803. (b) Wang, X. M.; Wang, P.; Fan, R. Q.; Xu, M. Y.; Qiang, L. S.; Wei, L. G.; Yang, Y. L.; Wang, Y. L. Solvatochromic and Application in Dye-sensitized Solar Cells of Sandwich-like Cd(II) Complexes: Supramolecular Architectures Based on N^1,N^3-bis[(6-methoxypyridin-2-yl)methylene]benzene-1,3-diamine. *Dalton Trans.* **2015**, *44*, 5179−5190.
(25) Zhao, X. L.; Tian, D.; Gao, Q.; Sun, H. W.; Xu, J.; Bu, X. H. A Chiral Lanthanide Metal−Organic Framework for Selective Sensing of Fe(III) Ions. *Dalton Trans.* **2016**, *45*, 1040−1046.
(26) (a) Wen, R. M.; Han, S. D.; Ren, G. J.; Chang, Z.; Li, Y. W.; Bu, X. H. A Flexible Zwitterion Ligand Based Lanthanide Metal−Organic Framework for Luminescence Sensing of Metal Ions and Small Molecules. *Dalton Trans.* **2015**, *44*, 10914−10917. (b) Liang, Y. T.; Yang, G. P.; Liu, B.; Yan, Y. T.; Xi, Z. P.; Wang, Y. Y. Four Super Water-stable Lanthanide−Organic Frameworks with Active Uncoordinated Carboxylic and Pyridyl Groups for Selective Luminescence Sensing of Fe^{3+}. *Dalton Trans.* **2015**, *44*, 13325−13330.

DOI: 10.1021/acs.inorgchem.6b01809
Inorg. Chem. 2016, 55, 10580−10586